Journal of Nuclear Materials 434 (2013) 158–161

Contents lists available at SciVerse ScienceDirect

Journal of Nuclear Materials

journal homepage: www.elsevier.com/locate/jnucmat

First-principles appraisal of solute ultra-fast diffusion in hcp Zr and Ti

R.C. Pasianot *, R.A. Pérez

Gerencia Materiales, CAC, CNEA, Avda. Gral. Paz 1499, 1650 San Martín, Argentina
CONICET, Avda. Rivadavia 1917, 1033 Buenos Aires, Argentina
Instituto Sabato, UNSAM/CNEA, Avda. Gral. Paz 1499, 1650 San Martín, Argentina

ARTICLE INFO

Article history:
Received 20 July 2012
Accepted 17 November 2012
Available online 29 November 2012

ABSTRACT

We revisit the ultra-fast diffusion characteristics of Fe, Co, Ni, and Cu solutes, in the hcp hosts Ti and Zr, by using Density Functional Theory. The energetics of several point defect configurations, deemed relevant for solute diffusion, is evaluated. The results support the long standing beliefs that the diffusing species is interstitial in nature, and that some kind of complexing is involved at low temperatures. Though quantitative agreement with experiment is difficult to assess, we show that a rather simple dissociative model is able to rationalize the observed trends, in particular, why the Arrhenius graphs are straight for Ti whereas, generally, they are curved downwards for Zr.

1. Introduction

Since the early 1970s there have been reports in the literature that certain metallic elements such as Fe, Co, Ni, and Cu, when dissolved in hexagonal Zr (and also Ni into Ti), behave as ultra-fast diffusers [1,2]; namely, their diffusion coefficients, close to the hcp-bcc transformation, are a million or larger times the host self-diffusion one. The observations referred mainly to well annealed, single-or large grain polycrystalline samples, thus essentially ruling out possible extrinsic effects. Such huge figures were interpreted as the outcome of an interstitial-like diffusion mechanism, idea that was thought to apply also to other earlier studied systems, such as Au into Pb [3]. Further experiments followed through the 1980s and 1990s, becoming clear that reliable extraction of the diffusion parameters, i.e., activation energy and pre-exponential factor, was a specially difficult task. Tracer hold up at the surface, back diffusion, general non-Arrhenius behavior of the profiles, were rather common issues, demanding non-standard corrective procedures at both, experimental and data analysis stages. Sample purity is an added concern to the list, as it was evident that a sort of defect complexing impacted solute diffusion at low temperatures. These problems plagued more dramatically the Zr host, where, at variance with Ti, all the solutes considered here but Cu, show a downwards curvature in the (Arrhenius) plots of ln$D$ vs $1/T$. Such a result, coupled to the limited extent of the hcp phase in the high temperature region, renders the estimation of diffusion parameters rather uncertain. In fact, literature values of the latter stem from applying a mix of experimental measurements and empirical correlations based on heuristic arguments [4].

Following the track of our previous works dealing mostly with Zr self-diffusion issues [5–7], first principles techniques are here applied to study the diffusion behavior of Fe, Co, Ni, and Cu, dissolved in hcp Ti and Zr. Acknowledging both, the uncertainties of the experimental measurements and the limitations of our own technique, the aim is not quantitative agreement or precise predictions but qualitatively correct trends, such as to contribute some light to the understanding of these peculiar systems. In particular, whether an interstitial migration mechanism is indeed supported by first principles calculations, and the reasons for the marked differences in the Arrhenius plots appearance among the two hosts. Thus, Section 2 details the systematics of the methodology followed to reach this goal, also advancing a summary of the calculations results. Section 3 discusses the internal consistency of those results and includes a comparison against the most reliable experiments. In this context, a rather simple model aimed at bringing into consistency experiments and calculations, is presented. The main points of our contribution are finally highlighted in Section 4.

2. Simulation method and results

First principles electronic structure calculations are applied in order to evaluate the (relative) energies of several standard configurations (specified later on) of the solute species into the host matrix. The calculations are performed with the Density Functional Theory (DFT) code SIESTA [8], that uses pseudopotentials and numerical, atomic-like, orbitals, for the wave-functions expansions. The generalized gradient approximation (GGA) as developed in [9] is employed for the exchange and correlation contribution to the energy. Consistency with the host metals of earlier works [7], demanded the construction of new pseudopotentials for Co, Ni, and Cu (norm-conserving, TM-type [10], including 3d and 4s states

* Corresponding author at: Gerencia Materiales, CAC, CNEA, Avda. Gral. Paz 1499, 1650 San Martín, Argentina. Tel.: +54 11 4839 6709; fax +54 11 6772 7362.
E-mail address: pasianot@cnea.gov.ar (R.C. Pasianot).

0022-3115/$ - see front matter © 2012 Elsevier B.V. All rights reserved.
http://dx.doi.org/10.1016/j.jnucmat.2012.11.029

with standard occupation into the valence, and core charge correction), together with corresponding optimized basis set functions (so called double-zeta polarized, DZP, 15 in all per atom). The hexagonal simulation cell consists of 96 lattice sites ($4 \times 4 \times 3$ units) and repeats periodically in space. A rather fine spatial mesh, 450.0 Ry cut-off, is used for the numerical integrations; in turn, reciprocal space is partitioned into a $3 \times 3 \times 3$ Monkhorst–Pack grid, and a smearing parameter of 0.15 eV (Fermi–Dirac scheme) is chosen for the integrations there. The atomic coordinates are relaxed via conjugate gradients up to a force level of 0.2 eV/nm, while keeping fixed cell size and shape. Previous researchers have simulated self-interstitials in Zr using the same cell size [11,12], where from an error of about 0.1 eV in formation energies might roughly be expected; it will become clear, however, that this does not affect our core qualitative conclusions. In summary, all running parameters are selected in order to attain a conservative degree of convergence.

The foreign atom is placed into the host lattice at various positions commonly considered on symmetry grounds and depicted in Fig. 1; these are: octahedral (O), substitutional (Sub), crowdion (C), basal octahedral (Bo), and basal crowdion (Bc). Besides those we add the off-lattice (Off), a slightly displaced atom from a lattice site suggested by our prior work on Fe. and a few dumbbell configurations between like and unlike species. Several of the energy minimizations included constraints, such as holding the atom at the C configuration; in no case however the remaining forces were larger than the chosen convergence level, thus assuring at least a stationary point in the energy.

The results of this procedure are gathered in Table 1, where for convenience the O configuration is taken as energy reference. A symbol appearing within the table indicates the configuration labelling the row is unstable with respect to that. Configurations left blank were simply not evaluated or are given elsewhere in the table. Figures are rounded to the second digit only for comparison reasons, no claim of such a precision is made. These calculations do not account for magnetism; in fact for a few cases we also performed magnetic calculations, and verified that differences in energy among the two types of calculations were negligible.

3. Discussion and comparison with experiments

There are several observations to be made regarding Table 1. First, energy differences among interstitial configurations are rather small, thus, diffusion through interstitial mechanisms is likely, provided these configurations are more stable than competing ones, such as the substitutional, that could possibly migrate via a standard vacancy mechanism. Second, taking the O interstitial as representative, it is clear that the Sub configuration is sizeably more stable in Ti, therefore, even if an interstitial migration mechanism is there operative, it will involve some promotion energy from Sub. Migration via a vacancy mechanism, but for the case of Cu into Ti, may not be competitive, since previous calculations have predicted activation energies of about 2.5 eV (e.g. [13,7]) whereas experiments report some 3.1 eV [14,15]. In the same context, the Sub configuration is increasingly more stable, for both hosts, along the sequence Fe, Co, and Ni; this is contrary to heuristic arguments based on atomic size [16], according to which, the smaller the atom the higher the chances of occupying interstitial sites. Third, it is particularly striking the large binding involved in the pair configurations (dumbbells), be they single species or mixed. Most likely these are relatively sessile structures since migration would involve coordinated motion and/or braking of the pair; thus, from the point of view of the fast diffuser, they would have a strong and negative impact on diffusion.

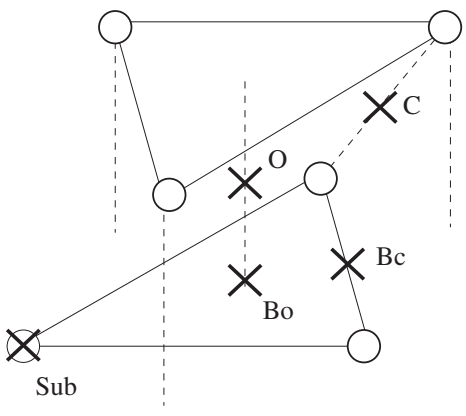

Fig. 1. A section of the hcp stacking showing most solute configurations studied.

Table 1
Calculated formation energy (eV) of point defects for solutes Fe, Co, Ni, and Cu, in hcp Zr and Ti hosts. The octahedral (O) configuration is taken as energy reference. X–X, Fe–X, and Co–X stand for pair clusters (dumbbells), X being the species in the column; the corresponding, isolated, octahedral configurations are used as energy reference in this case.

	Zr				Ti			
	Fe	Co	Ni	Cu	Fe	Co	Ni	Cu
O	0.00	0.00	0.00	0.00	0.00	0.00	0.00	0.00
Sub	0.39	0.10	−0.53	−1.58	−0.85	−1.13	−2.19	−2.76
C	0.13	0.21	0.33	0.25	−0.14	0.01	−0.14	−0.07
Bo	0.33	0.27	0.21	0.21	0.12	0.15	−0.27	−0.06
Off	0.11	−0.04	Sub	Sub	−0.98	Sub	Sub	Sub
Bc	0.15	0.12	0.12	Bo	−0.05	0.02	−0.25	
X–X	−1.60	−1.93	−2.38	−3.00	−2.71	−3.04	−3.82	
Fe–X		−1.70	−1.91	−2.20		−2.87	−3.31	
Co–X			−2.09					

Fig. 2 shows experimental diffusion data for Fe [17], Co [18], Ni [19,20], and Cu [2] solutes, in hcp Zr single-crystals. The symbol $\|/\perp$ stands for direction parallel/perpendicular to the c axis; where appropriate, the $\alpha \leftrightarrow \beta$ transformation temperature (1136 K) is indicated. The line labelled "Fitted" is a fit by us using a four-parameters curve to be commented later on. But for Cu, the straight lines labelled Q are added by us in order to convey an idea of slope. Only $D_{\|}$ is shown for Fe, because it has been measured in a wider T range; regarding Co, the (close to) $D_{\perp}$ measurement is stated as more reliable by the original author. A salient feature of the plots is the downward curvature for the cases of Fe, Co, and probably Ni; Cu shows a standard, normal, behavior. Notice however that, at variance with the other cases, the latter includes only a single point below (and close) 900 K. It is also worth mentioning that Co data is interpreted as broken into two pieces, below and above 900 K, in the original Ref. [18]. Sample purity varies, but as a guide we can take the Fe case, namely, Fe, Co, and Ni contents are quoted as 100, 30, and 10 at ppm, respectively. In all cases diffusion is reported to be anisotropic, with $D_{\|} > D_{\perp}$.

Regarding the Ti host, experimental diffusion data for Fe, Co, and Ni, is gathered in Table 2; no data is available for Cu. All the Arrhenius plots were reported as normal, straight lines; the poly-crystal ("Poly") measurements are extensions of single-crystal ones, to lower temperatures. In this context, the Fe case is in fact for a Ti-0.029 at.% Fe alloy, and the two lowest temperature points, 795 and 800 K, drop somewhat from the straight line extrapolation of higher temperatures. In contrast, the poly-crystal Co experiment [21] was specifically designed to test for downward curvature, effect that was not observed. Sample purity for the latter was Fe < 150, Ni < 50, Co < 10 at ppm; in the remaining experiments the Fe content was <10 at ppm. Regarding diffusion anisotropy, the same result as for Zr holds, namely, $D_{\|} > D_{\perp}$ for all cases.

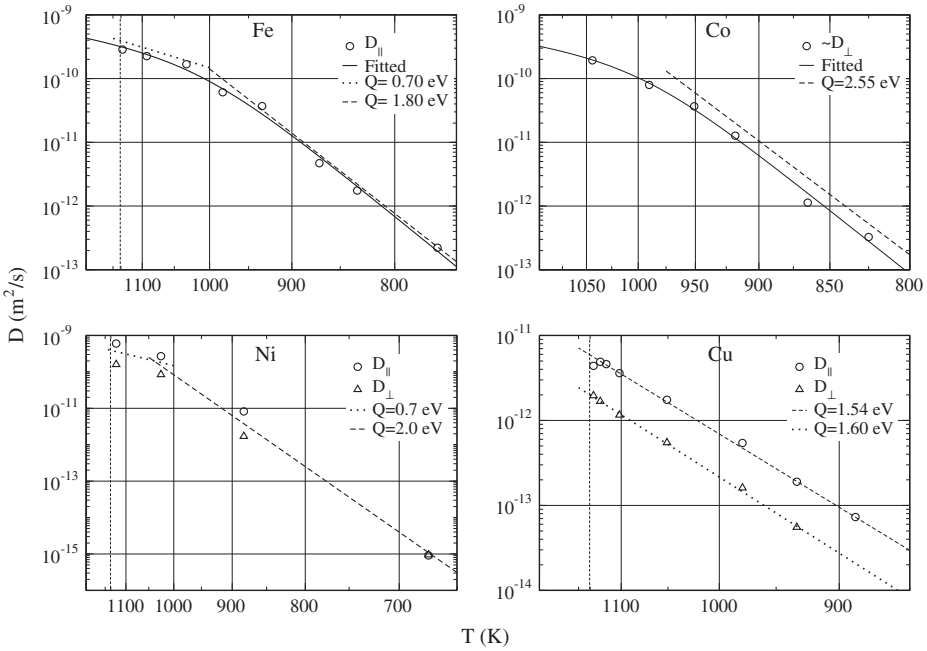

Fig. 2. Experimental data for diffusion of Fe, Co, Ni, and Cu solutes in hcp Zr. See main text for details.

Table 2
Measured solute diffusion parameters in hcp Ti.

Solute	Direction	Q (eV)	D_0 (m^2/s)	T range (K)	Ref.
Fe	‖	1.17	4.7×10^{-7}	877–1136	[25]
Fe	⊥	1.50	6.4×10^{-6}	877–1136	[25]
Fe	Poly	1.30	1.0×10^{-6}	795–1082	[26]
Co	‖	1.19	1.9×10^{-6}	871–1135	[27]
Co	⊥	1.31	3.2×10^{-6}	871–1135	[27]
Co	Poly	1.32	3.0×10^{-6}	619–823	[21]
Ni	‖	1.91	5.8×10^{-6}	875–1100	[28]
Ni	⊥	1.97	4.8×10^{-6}	875–1100	[28]

Let us now contrast calculations vs experiments. Perhaps the best established result of the latter is the anisotropy of diffusion, $D_\parallel > D_\perp$; it is however the most speculative to analyze from the former point of view. We can only argue on the basis of the stationary energy points for the interstitial configurations of Table 1 (no exhaustive search of local minima/saddles was performed), trying to judge whether $Q_\parallel < Q_\perp$ holds. Such a correlation, however, may be flawed as the measurement for Cu into Zr suggests (only exception). Heuristic arguments based on atomic size [4] suggest the O configuration as the stable one and Bo to be the (easiest) saddle. Our calculations are not necessarily consistent with this view. For the Zr host, O is indeed predicted as the lowest energy interstitial configuration; the saddle however, seems more related to Bc, lower in energy than Bo for all cases but Cu (where Bc decays to Bo). Bc would lead to easy migration along the hollow triangular channels of the ABAB stacking, thus to $Q_\parallel < Q_\perp$. Notice however the case of Fe, where C is slightly lower in energy than Bc, migration through C occurs purely on the basal plane, thus implying $Q_\parallel > Q_\perp$. Preference for reduced symmetry configurations finds no explanation within a hard spheres model, it is probably a bonding effect stemming from the d orbitals; incidentally, the d shell in Cu gets completed. In Ti, such a preference is still stronger, since the lowest energy configuration may not be O any more. We go from C for the Fe case, to about a degeneracy O–C–Bc for the Co case, to a clear Bc for Ni; the Cu case was not pursued further in view of the deeply bound Sub configuration. With this scenario, assessing activation energy relationships becomes more speculative than in Zr, since one can easily envisage fully 3-dimensional migration paths built out of sequences of C and Bc.

Regarding the activation energies themselves, our calculations predict, roughly, an overall value of 0.3 eV for interstitial migration (c.f. Table 1). Quoted values in [4] for Fe and Ni in Zr are 0.80 and 0.68 eV respectively. Apparently, though compatible, calculations somewhat underestimate experiments. Intermediate Q's, such as those of Cu in Zr, and Fe and Co in Ti (c.f. Fig. 1 and Table 2), need further explanations, as well as the rather large Q's of Fe, Co, and Ni in Zr at low temperatures. To account for this variety of behaviors, we propose a variant of the dissociative model [22,3] where the migrating species may adopt any of three states: (1) a highly mobile interstitial, (2) (relatively) immobile substitutional, and (3) (relatively) immobile trapped at impurities. State (2) is supported by our results for the Sub configuration, whereas state (3) is supported by the results for the pair configurations. A word of caution is in order at this point, namely, the specific processes involved in tracer trapping can be very complex and difficult to capture by any modelling, least by our rather crude approach below. In this sense, the large binding energies of the pair configurations of Table 1, should be viewed as evidence that foreign atoms can indeed behave as strong traps, though the real mechanism may not be pair formation. Thus, calling x the total tracer concentration, and x_1, x_2, x_3, respectively, the concentrations of the just mentioned three states, the effective diffusion coefficient D will be given by,

$$D = \frac{x_1}{x}\, D_0\, e^{-Q_1/kT}. \tag{1}$$

On the other hand, the respective statistical weights, w_i, can be taken as,

$$\begin{aligned} w_1 &= 1 \\ w_2 &= e^{G_2/kT} \\ w_3 &= y\, e^{G_3/kT}, \end{aligned} \tag{2}$$

where y stands for the impurity concentration, and G_2 and G_3 are the free energy changes upon conversion from states (2) and (3) to state (1) respectively. Thus, replacing in Eq. (1),

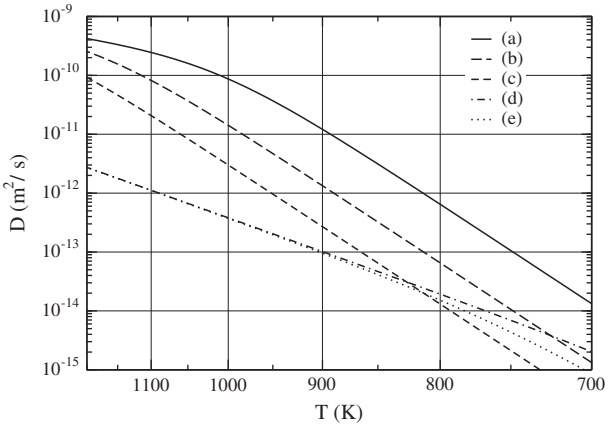

Fig. 3. Diffusivity behavior according to Eq. (3). (a): $D_0 = 5.28 \times 10^{-8}$ m^2/s, $Q_1 = 0.42$ eV, $G_2 = 0.0$ eV, $y = 1.17 \times 10^{-7}$, and $G_3 = 1.46$ eV (data for Fe in Zr). (b): Same as (a) but $10 \times y \to y$. (c): Same as (a) but $50 \times y \to y$. (d): Same as (a) but $G_2 = 0.6$ eV. (e): Same as (b) but $G_2 = 0.6$ eV.

$$D = D_0 \frac{e^{-Q_1/kT}}{(1 + e^{G_2/kT} + y\ e^{G_3/kT})}. \quad (3)$$

The above expression predicts that D may show up to three different regimes, depending on which term in the denominator prevails. Taking energies for free energies and noting that Table 1 suggests $G_2 < G_3$, the intrinsic regime will occur at high temperatures, the one dominated by the substitutional species will happen at intermediate temperatures, and the effect of impurities will be seen at low temperatures. The presence or absence of any of those is system specific and depends on the temperature range being studied.

From this viewpoint, the experimental results for Fe, Co, and Ni dissolved in Zr, represent a transition from the intrinsic regime, or a mixture with the substitutional one, to the impurity dominated regime, due to relatively small G_2 values. In this spirit, we performed a least squares fit of the Fe and Co into Zr experimental data to Eq. (3) by putting $G_2 = 0.0$ and taking D_0, Q_1, y, and G_3 as free parameters, "Fitted" label of Fig. 2. The specific values obtained for Fe were $D_0 = 5.28 \times 10^{-8}$ m^2/s, $Q_1 = 0.42$ eV, $y = 1.17 \times 10^{-7}$, and $G_3 = 1.46$ eV. But for y, these parameters are roughly within expectations, namely, Q_1 and G_3 from the interstitials and dumbbells energies of Table 1 respectively, D_0 e.g. from the reported values in Table 2 for Ti. On the other hand, parameter y seems too low when confronted with the impurity contents quoted previously. We recall, however, our cautions regarding the precise trapping mechanism being operative, and note in passing that such a value is not far from a like 4.6×10^{-6} derived in [23] for vacancy trapping in the context of Zr self-diffusion data [24]. As a further consistency check, in Fig. 3 we take this Fe in Zr curve (a) and increase the impurity content, y, by factors of 10, (b), and 50, (c). It is readily observed that the curve straightens quickly and diffusivity diminishes; this is precisely what has been observed for Fe in [17] after comparison of the (pure) Zr single-crystal data against data for a polycrystalline alloy Zr-0.28 at.% Fe (733–1070 K).

The case of Cu in Zr and all the remaining ones involving Ti, are substitutional dominated, because of a sizeable G_2 value. To show this effect, in Fig. 3 we again take curve (a) and increase G_2 to a mild 0.6 eV, (d); moreover, in (e) we have taken the latter and increased the impurities 10 times. Two features are born out by this exercise: (i) the presence of a substitutional configuration straightens the plot very fast and (ii) further impurity increase can hardly make any difference. (i) is nothing but our claim; regarding (ii) it has been observed in [26] that Fe data for a Ti-0.029 at.% Fe polycrystalline alloy, nicely align with the random average of $D_\parallel$ and $D_\perp$ when diffusing in (pure) single-crystal Ti. Moreover, the low temperature experiment performed in [21] for Co into Ti, using polycrystalline samples of about 10 times the Fe content of the single-crystal samples of Ref. [27], not only shows a straight plot but also a very good match to the latter.

4. Conclusions

Though quantitative agreement is difficult to judge from both sides, theory and experiment, we have shown that first-principles calculations can be a powerful tool to rationalize experimental trends. Moreover, they lend further support for an interstitial migration mechanism of the studied solutes in Zr as well as in Ti. The impact of the competing substitutional configuration on the effective activation energy has been demonstrated, and, particularly, the strong binding effects and concurrent diffusion slow down, that impurities may have. Last, chemical bonding effects responsible for departures from expected behaviors based on atomic/ionic sizes, have been hinted at; the matter however deserves more in-depth research.

Acknowledgement

The support from CONICET PIP 804/10 is gratefully acknowledged.

References

[1] G.M. Hood, R.J. Schultz, Philos. Mag. 26 (1972) 329.
[2] G.M. Hood, R.J. Schultz, Phys. Rev. B 11 (1975) 3780.
[3] W.K. Warburton, Phys. Rev. B 11 (1975) 4945.
[4] G.M. Hood, J. Nucl. Mater. 159 (1988) 149.
[5] R.A. Pérez, M. Weissman, J. Nucl. Mater. 374 (2008) 95.
[6] R.C. Pasianot, R.A. Pérez, V.P. Ramunni, M. Weissmann, J. Nucl. Mater. 392 (2009) 100.
[7] R.C. Pasianot, R.A. Pérez, Physica B 407 (2012) 3298.
[8] J.M. Soler, E. Artacho, J.D. Gale, A. García, J. Junquera, P. Ordejón, D. Sánchez-Portal, J. Phys. Condens. Matter 14 (2002) 2745.
[9] J.P. Perdew, K. Burke, M. Ernzerhof, Phys. Rev. Lett. 77 (1996) 3865.
[10] N. Troullier, J.L. Martins, Phys. Rev. B 43 (1991) 1993.
[11] Ch. Domain, A. Legris, Philos. Mag. 85 (2005) 569.
[12] F. Willaime, J. Nucl. Mater. 323 (2003) 205.
[13] G. Vérité, F. Willaime, C.C. Fu, Solid State Phenom. 129 (2007) 75.
[14] M. Köpers, C. Herzig, M. Friesel, Y. Mishin, Acta Mater. 45 (1997) 4181.
[15] G.M. Hood, H. Zou, R.J. Schultz, N. Matsura, J.A. Roy, J.A. Jackman, Defects Diff. Forum 143–147 (1997) 49.
[16] G. Hood, J. Nucl. Mater. 139 (1986) 179.
[17] H. Nakajima, G.M. Hood, R.J. Schultz, Philos. Mag. B 58 (1988) 319.
[18] G.V. Kidson, Philos. Mag. A 44 (1981) 341.
[19] G.M. Hood, R.J. Schultz, Mater. Sci. Forum 15–18 (1987) 475.
[20] G.M. Hood, R.J. Schultz, Proc. 8th Int. Symp. on Zirconium in the Nuclear Industry, ASTM, 1989, pp. 435.
[21] R.A. Pérez, F. Dyment, Philos. Mag. A 71 (1995) 965.
[22] P.C. Frank, D. Turnbull, Phys. Rev. 104 (1956) 617.
[23] W. Frank, Defects Diff. Forum 66–69 (1990) 387.
[24] J. Horváth, F. Dyment, H. Mehrer, J. Nucl. Mater. 126 (1984) 206.
[25] H. Nakajima, M. Koiwa, S. Ono, Scripta Metall. 17 (1983) 1431.
[26] H. Nakajima, K. Yusa, Y. Kondo, Scripta Mater. 34 (1996) 249.
[27] H. Nakajima, M. Koiwa, Trans. Jpn. Inst. Met. 24 (1983) 655.
[28] H. Nakajima, S. Maekawa, Y. Aoki, M. Koiwa, Trans. Jpn. Inst. Met. 26 (1985) 1.